Supporting information

Macroscopic pictures of complex coacervates

Method:

The turbidity resulting from complexation between positively charged lysozyme and negatively charged HAMA or CSMA was studied and photographed. HAMA and CSMA solutions (5% w/w) or HAMA and CSMA microgels (1mg/ml) were prepared in buffers of 20 and 170 mM ionic strength. A 0.5 mL solution of 4mg/ml lysozyme in a buffer was then added to a vial filled with 0.5mL of GAG containing buffer. Samples were subsequently checked for turbidity and pictures were taken after 5 minutes.

Results:

Both CSMA and HAMA formed complexes with lysozyme in a 20 mM ionic strength buffer (indicated by the milky turbid appearance), the mixture containing CSMA was clearly more turbid than the HAMA sample. This stronger turbidity likely indicates stronger interaction between GAG and lysozyme, implicating that CS exhibits stronger complexation with lysozyme than HA due to the presence of the additional negatively charged sulfate moiety per disaccharide unit of this polymer. In SI-FIG1B the same experiment done in 170 mM ionic strength buffer showed that the HAMA mixture did not show signs of complex coacervation, whereas the CSMA mixture still turned turbid but appreciably less so when compared to the 20 mM ionic strength buffered CSMA – lysozyme mixture. All mixtures immediately turned completely transparent upon agitation, indicating that the complexes became solubilized. Several literature sources report on complex coacervation between soluble polymer HA/CS and lysozyme [1-4]. It is generally found for both GAGs that the introduction of protein to a GAG in a low ionic strength medium causes complex coacervation based on electrostatic attraction. A study performed by Moss *et al* on both hen egg white lysozyme and lysozyme extracted from cartilage also reported that both HA and CS can bind large amounts of lysozyme in low ionic strength conditions. Importantly, all studies cited did not find any complexation to occur between HA and lysozyme and only limited binding between CS and lysozyme in conditions where the ionic strength of the medium approached physiological levels.

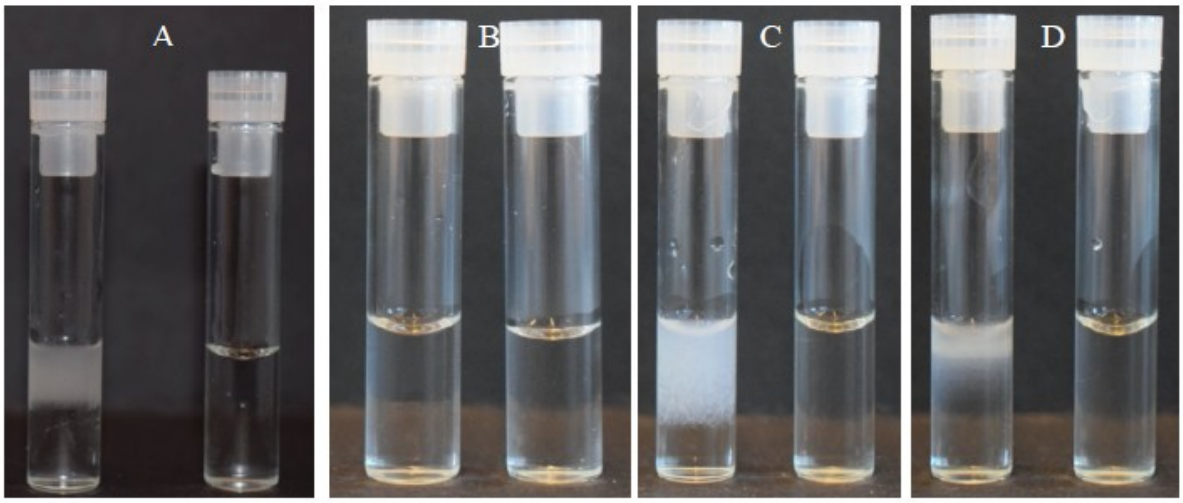

SI Fig. 1: Macroscopic pictures of complexes between negatively charged glycosaminoglycans and positively charged lysozyme. A: HAMA mixed with lysozyme (left) and without lysozyme (right) in 20 mM ionic strength buffer B: HAMA mixed with lysozyme (left) and without lysozyme (right) in 170 mM ionic strength buffer, C: CSMA mixed with lysozyme (left) and without lysozyme (right) in 20 mM ionic strength buffer and D: CSMA mixed with lysozyme (left) and without lysozyme (right) in 170mM ionic strength buffer.

Microfluidic device design

A microfluidics set-up was developed as follows. A dual syringe pump (model 33, Harvard Apparatus) was used to allow two different constant flows. Disposable syringes with luer-lock fittings (typically a 1mL syringe for the water phase and a 50 mL syringe for the oil phase) were used to inject the two different phases and were connected to 1/16th inch OD Teflon tubing by screwing their luer tips into the tubing adapters. Tubing containing the external and the internal phase were let to converge into a customized polyethyletherketone (PEEK) T-junction (Sigma Aldrich). The three T-junction inlets (original ID = 0.020 inch) were drilled out with a micro-drill to an ID roughly equal to 0.040 inch to facilitate high fluid flows. The tube containing the external phase was connected to the inlet of the T-junction via a nut and ferrule (orange fluid stream in Figure 1). To form micrometer sized droplets of the internal phase, the extremity of the tube containing this phase was equipped with a blunt *Nanofil*® needle (115 µm ID, World Precision Instruments, Germany). To generate a leak-free connection between the tube and the needle, the needle holder was partially inserted into a 1 cm-long tube of chemically resistant, polyolefin-based heat shrink (OD diameter of 3/64th inch) and was held above a hot soldering iron to shrink the tubing around the needle. This was then inserted into the 1/16th inch tube creating a snug fit. To create a co-flowing geometry, a nut and ferrule were fitted onto the tubing and connected to one of the two straight inlets of the PEEK T-junction. The last opening of the T-junction was connected via a nut to 1/8th inch OD tubing acting as the receiving channel for the generated droplets. The droplets were then collected in a petri-dish partially filled with the external oil phase.

Fabrication of microgels – viscosity of continuous and disperse fluids

Method:

The viscosity of the different fluids used as continuous phase and HAMA and CSMA solutions (i.e. disperse phase solutions) before and after filtration were measured using a Dynamic Hybrid Rheometer DHR-2 (TA Instruments) equipped with a Peltier plate. A 20 mm 1° steel cone (27 µm truncation gap) was used. Flow peak measurements at 25 °C was performed with a frequency of 100/s for 2 minutes with 20 measurements. (see table SI.1)

Results:

SI Table 1: viscosities of fluids used in the microfluidic set-up

Material	Viscosity before filtration (in mPa.s)	Viscosity after filtration (in mPa.s)
Mineral oil + 8 wt % SPAN80	31 ± 4	31 ± 4
2.5 wt % HAMA + 0.5 wt % IG2959 in H_2O	12 ± 1	13 ± 1
5 wt % HAMA + 0.5 wt % IG2959 in H_2O	50 ± 1	54 ± 1
5 wt % CSMA + 0.5 wt % IG2959 in H_2O	24 ± 1	33 ± 1

GAG microgel protein absorption and distribution studies using FITC-lysozyme

To visualize the kinetics of lysozyme absorption by 5% HAMA and 5% CSMA microgels, a mixture of FITC labeled lysozyme and unlabeled protein was incubated with the microgels. A 1:20 FITC-lysozyme: lysozyme (wt/wt) mixture in 20 mM ionic strength buffer was used. The total concentration of both labeled and unlabeled lysozyme in each mixture was 2 mg/mL. In SI Fig. 2A-D the lysozyme uptake of 5% HAMA microgels is shown over time and both bright field and fluorescence confocal images were taken simultaneously (animated movies can be found in the SI [supplemental movies 1 and 2). Clearly, after 5 (SIFig.2A) and 15 min (SIFig.2B) the protein is starting to infiltrate the microgels. When comparing the bright field images to the fluorescence images it can be seen that the parts of the microgel that have been filled up by the protein were are also changing in terms of contrast. This is likely due to a change in refractive index as a result of the increase in local protein/polymer concentration (deswelling of the microgels, also see Fig.7 and SIFig 2), resulting in enhanced contrast. After ~45

min (see SIfig.2D) the protein has reached the inner core of the microgels, and had distributed homogeneously over the matrix. In general the CSMA microgels undergo the same transformation as their HAMA counterparts, except for two notable differences (see supplemental movie SI.2). While the HAMA microgels were fully saturated with lysozyme after 60 min, the CSMA microgels needed ~12 h to completely load and deswell. This slower loading kinetics is similar to what is reported in section 3.3. and is likely related to the fact that the high loading of lysozyme in CSMA started at the gel-water interface, where it substantially dehydrated the hydrogel structure, reducing the pore size of the gel network which in turn slowed down further diffusion of protein into the matrix. Furthermore, due to their lower initial density (the CSMA microgels were 700 μm in diameter as compared to 500 μm of the same wt% HAMA microgels) and their subsequent high loss of water, the CSMA microgels jetted around in the well in which they were measured for the duration of the experiment. Presumably this movement was fueled by the constant expulsion of water as the lysozyme replaced it in the hydrogel matrix. Due to the subsequent collisions, formation of some debris over time was observed, likely due to mechanical erosion, as discussed in section 3.2.

SI Fig.2A

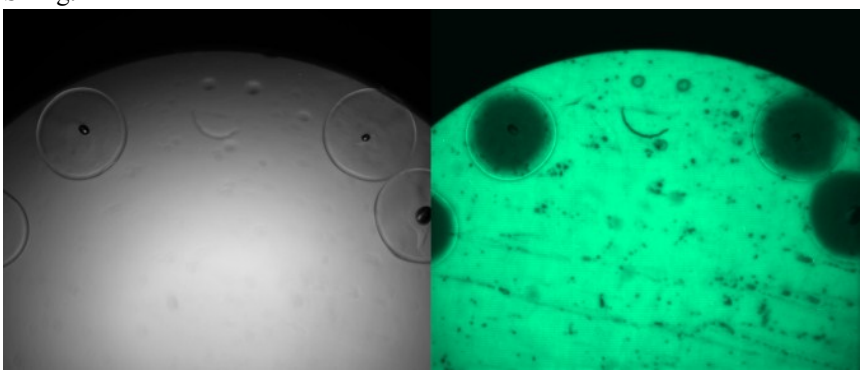

2B

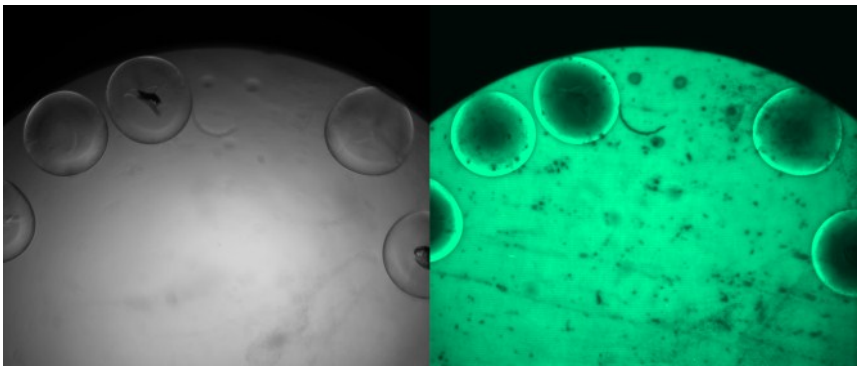

2C

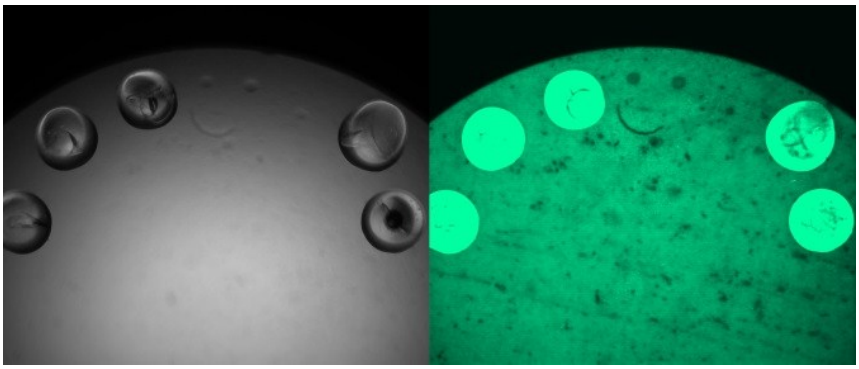

2D

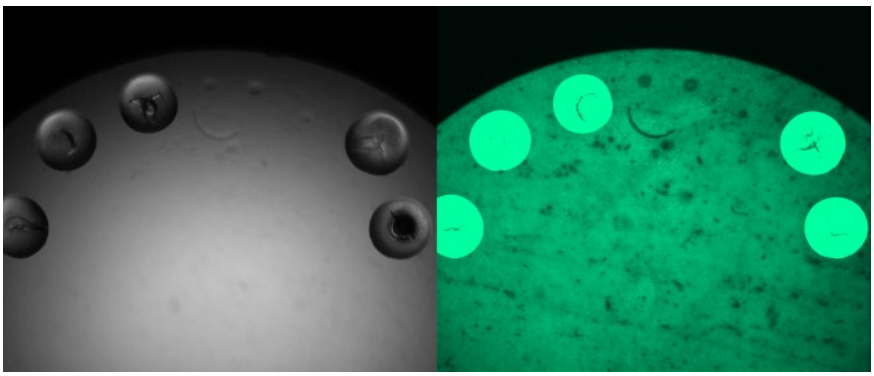

SI Fig.2. Confocal images of uptake of a mixture of FITC-lysozyme and lysozyme in 5 wt% HAMA microgels in low (20mM) ionic strength buffer. Micrographs (4x magnification) were taken respectively after 5 (2A), 15 (2B) 45 (2C) and 60 (2D) min.

Fluorescence confocal microscopy images of CSMA particles in thermogel and CSMA/thermogel blends
Protein distribution within composites and blends was studied using FITC-labeled lysozyme and a confocal fluorescence microscope (Yokogawa cell voyager) equipped with a 405nm laser and a 4x objective. For the loading of composite and blends, a 1:20 FITC-lysozyme: lysozyme w/w mixture in 20 mM ionic strength buffer was used. FITC-lysozyme-lysozyme mixtures were loaded and fabricated into hydrogel disks as reported in 2.10 and placed in a well plate.

Results:

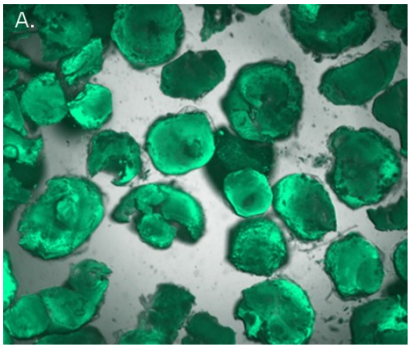

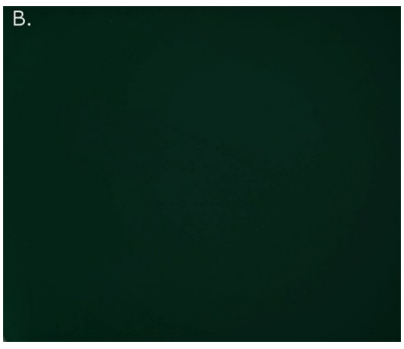

SI Fig. 3 : (A) Confocal microscopic pictures of CSMA microgels loaded with FITC-lyszoyme: lysozyme mixture embedded in thermogel and (B) FITC-lyszoyme:lysozyme mixture complexed with CSMA free polymer crosslinked with thermogel (i.e. the blend formulation).

FRAP recovery curves for photobleached GAG microgels loaded with FITC-lyszoyme:lysozyme mixture in different buffers.

The data gathered were first normalized and the FRAP curves were subsequently analyzed using FRAPanalyzer software [5-7]. The FRAP curves were fitted utilizing an equation for a circular bleach area and diffusion-dominated recovery to yield a diffusion coefficient in $\mu m^2.s^{-1}$ as originally derived by Soumpasis[8]. Corresponding FRAP curves and equations used for normalization and fitting are reported here.

$$I_{normalized}(t) = \frac{I_{spot}(t) - I_{background}(t)}{I_{pre-bleach\ spot}} \qquad \text{eq.SI1}$$

Where $I_{normalized}$ is the normalized fluorescence intensity at time point *t*, I_{spot} is the measured average intensity inside the bleached spot; and $I_{background}$ is the measured average background intensity. $I_{pre\text{-}bleach\ spot}$ is the average intensity in the designated spot before bleaching and after subtraction of $I_{background}$. :

$$FRAP(t) = a_0 + a_1 * e^{\frac{\tau}{2(t-t_{bleach})}} * \left(I_0\left(\frac{\tau}{2(t-t_{bleach})}\right) + I_1\left(\frac{\tau}{2(t-t_{bleach})}\right)\right),\ \tau = \frac{w^2}{D} \qquad \text{eq.SI2.}$$

Here, I_0 and I_1 are modified Bessel functions and τ is governed by the radius of the bleached spot (*w*) in μm and the diffusion coefficient (*D*) in $\mu m^2.s^{-1}$. The parameters t and t_{bleach} represent the time point measured and the time of bleaching in s respectively. Two normalizing coefficients (a_0 and a_1) were introduced to account for the non-zero intensity at bleach moment and incomplete recovery. *FRAP(t)* represents the normalized fluorescence intensity at timepoint *t*. FRAP curves are reported in SIFig.4 and 5.

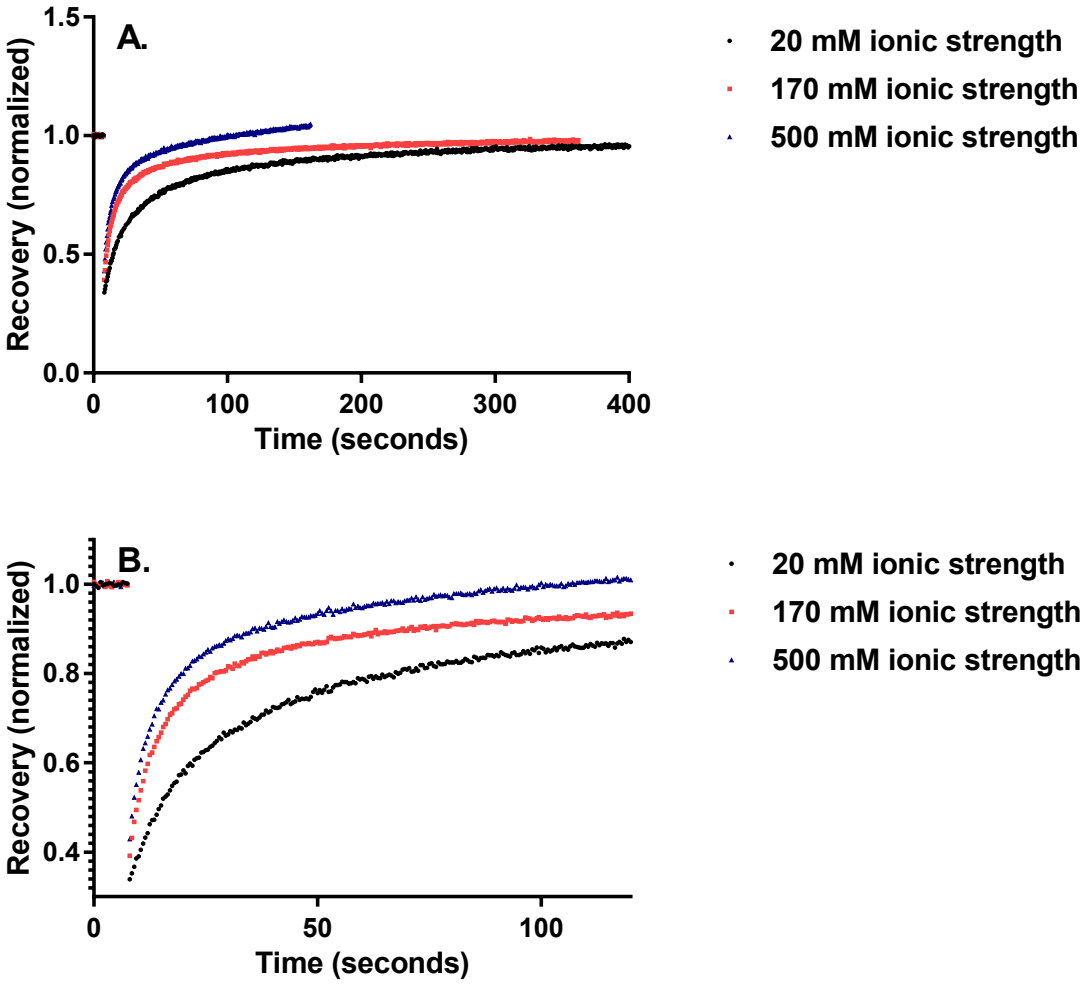

SI FIg.4A FRAP recovery curves of 5 wt% HAMA microgels loaded with FITC-lysozyme:lysozyme mixture in three different release buffers, Fig.4B shows a zoom-in of the recovery curve.

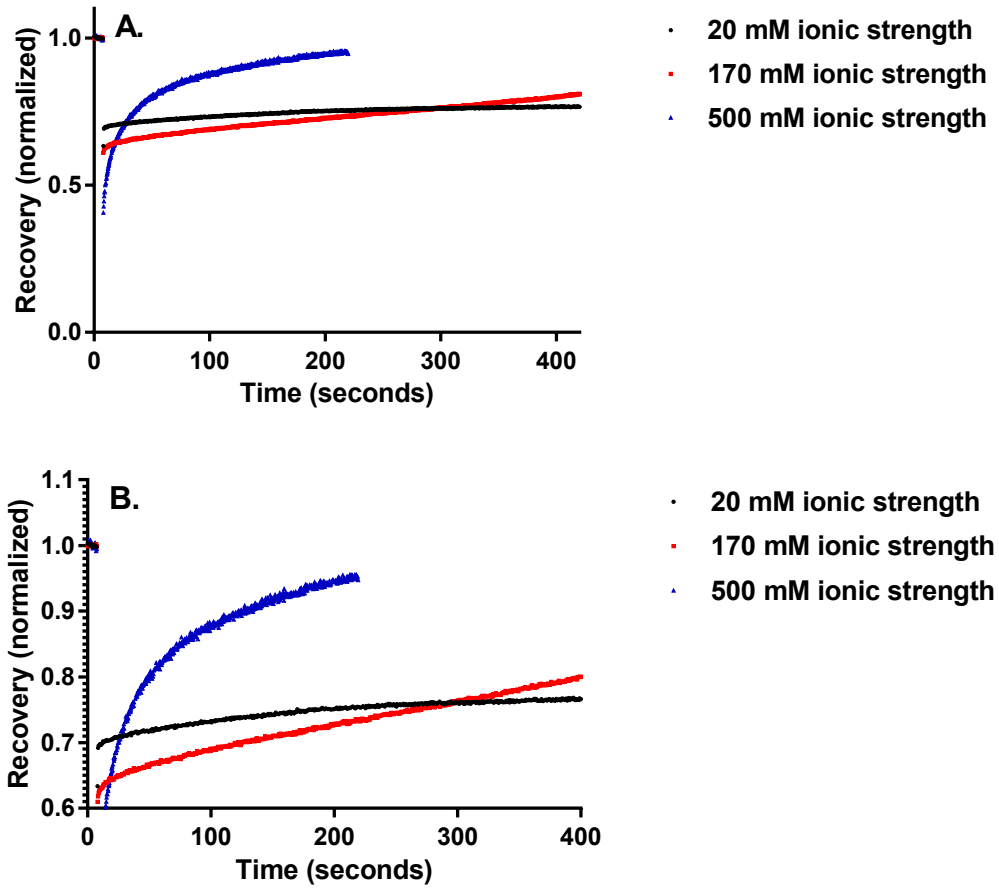

SI Fig.5A FRAP recovery curves of 5 wt% CSMA microgels loaded with FITC-lysozyme:lysozyme mixture in three different release buffers, Fig.5B shows a zoom-in of the recovery curve.

Lysozyme activity assay

Method:

The enzymatic activity of released lysozyme was determined via a turbidity-assay, based on the decrease in optical density of a suspension of *Micrococcus lysodeikticus* bacterium due to the hydrolysis of its outer membrane caused by lysozyme [9,10]. Briefly, samples containing released lysozyme were diluted to match the concentration of a native lysozyme stock solution (30 µg/ml in PBS), which was used as a positive control. Volumes of 5 µl of sample or control were pipetted into individual wells. Next, 195 µl of *Micrococcus lysodeikticus* bacterium suspension (0.2 mg/ml in 22 mM phosphate buffer, pH = 6.2) was rapidly added to each well. The plate was shaken for 1 minute and the absorbance was measured at 450 nm over 5 minutes. The resulting curves were fitted with linear regression, and their slopes (proportional to lysozyme activity) were calculated and normalized to the slope of the linear curve of the native lysozyme.

Results:

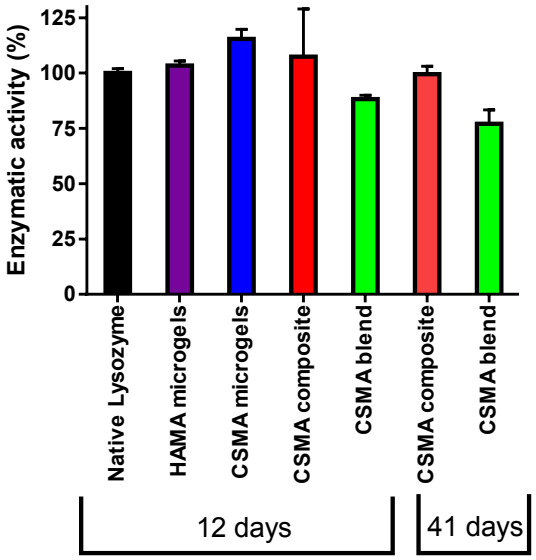

SI fig.6: Lysozyme activity assay as performed for all investigated formulations, either after 12 or 41 days.

References:

1. J. J. Water, M. M. Schack, A. Velazquez-Campoy, M. J. Maltesen, M. van de Weert and L. Jorgensen, *European Journal of Pharmaceutics and Biopharmaceutics*, 2014, **88**, 325-331.
2. J. M. Moss, M.-P. I. Van Damme, W. H. Murphy and B. N. Preston, *Archives of Biochemistry and Biophysics*, 1997, **348**, 49-55.
3. M. Vandamme, J. Moss, W. Murphy and B. Preston, *Archives of Biochemistry and Biophysics*, 1994, **310**, 16-24.
4. I. Morfin, E. Buhler, F. Cousin, I. Grillo and F. Boué, *Biomacromolecules*, 2011, **12**, 859-870.
5. A. Halavatyi, S. Medves, C. Hoffman, V. Apanasovich, M. Yatskou and E. Friederich, 2008.
6. T. K. L. Meyvis, S. C. De Smedt, P. Van Oostveldt and J. Demeester, *Pharmaceutical Research*, 1999, **16**, 1153-1162.
7. H. Deschout, K. Raemdonck, J. Demeester, S. C. De Smedt and K. Braeckmans, *Pharmaceutical Research*, 2014, **31**, 255-270.
8. D. M. Soumpasis, *Biophysical Journal*, 1983, **41**, 95-97.
9. R. A. Kern, M. J. Kingkade, S. F. Kern and O. K. Behrens, *Journal of Bacteriology*, 1951, **61**, 171-178.
10. T. B. Toro, T. P. Nguyen and T. J. Watt, *MethodsX*, 2015, **2**, 256-262.